MSW MANAGEMENT -Multidisciplinary, Scientific Work and Management Journal
ISSN: 1053-7899
Vol. 35 Issue 2, 2025, Pages: 2202-2211

Scoring System for Predicting Ovarian Necrosis in Adnexal Torsion Using an Ultra-Short, Optimized MRI Protocol

Dr Divyadarshny S[1*], Dr Jyothsana Harini Suma S P[2], Dr Alex Daniel Prabhu[3], Dr Sathyanarayanan V[4], Dr Einstein A[5]

1. Dr Divyadarshny S, Final year postgraduate,
Department of Radiology, Chettinad Hospital and Research Institute, Chettinad Academy of Research and Education, Kelambakam-603103, Tamil Nadu, India
Email ID: daringnddashing@gmail.com
ORCID ID: 0009-0007-8251-5129
2. Dr Jyothsana Harini Suma S P, Consultant Radiologist,
Sree Siva Hospital, Coimbatore, Tamil Nadu, India
Email ID: harinijyo227@gmail.com
3. Dr Alex Daniel Prabhu, Professor & HOD,
Department of Radiology, Chettinad Hospital and Research Institute, Chettinad Academy of Research and Education, Kelambakam-603103, Tamil Nadu, India
Email ID: dralexdaniel@hotmail.com
4. Dr Sathyanarayanan V, Senior Resident,
Department of Radiology, Chettinad Hospital and Research Institute, Chettinad Academy of Research and Education, Kelambakam-603103, Tamil Nadu, India
Email ID: sathyanarenhere@gmail.com
Mobile number: 7299535049
5. Dr Einstein A, Professor,
Department of Radiology, Chettinad Hospital and Research Institute, Chettinad Academy of Research and Education, Kelambakam-603103, Tamil Nadu, India
Email ID: einstien.raju@gmail.com
***Corresponding author**

ABSTRACT:

Background:

Adnexal torsion constitutes an acute gynecological condition, and diagnostic imaging modalities are instrumental in its timely and accurate identification. Magnetic Resonance Imaging (MRI) is distinguished by its enhanced soft tissue discrimination capabilities, yielding comprehensive data pertaining to the adnexal structures, thereby facilitating the precise identification of torsion and its concomitant complications.

Methods:

This hospital-based, cross-sectional study employed 50 participants comprising females aged between 10 and 50 years, with ovarian or adnexal torsion established via Magnetic Resonance Imaging (MRI). The study's data collection was performed from February 2024 to February 2025, after obtaining Ethical Committee approval.

Results:

The mean duration for a conventional magnetic resonance imaging (MRI) examination was 36.1 minutes, whereas the optimized MRI protocol significantly reduced this to 6.2 minutes ($p<0.05$). The average participant age was determined to be 39.5 years. The etiology of torsion was known in 74% of cases, with 83.8% attributed to benign conditions and 16.2% to malignant pathologies. Within the benign category, functional cysts represented the primary etiological factor (29%), whereas endometrial adenocarcinoma constituted the foremost malignant contributor (50%). MRI findings with hypointensities in the pedicle, cyst wall, perifollicular regions, and stroma exhibited a significant association with hemorrhagic necrosis. The ultra-short MRI protocol predicted 93.1% of necrotic cases with a score of 2 or higher on the established MRI scoring system. This methodology exhibited superior diagnostic performance, characterized by a sensitivity of 93.1%, a specificity of 90.5%, and a positive predictive value of 93.1%.

Conclusion:

The ultra-short, optimized MRI protocol proves to be an exceptionally valuable diagnostic modality for the prediction of hemorrhagic necrosis in adnexal torsion.

Keywords:

Adnexal torsion, Magnetic resonance imaging, Optimized MRI protocol, Ovarian necrosis, Scoring System

INTRODUCTION:

Adnexal torsion constitutes an urgent gynecological condition defined by the rotation of the ovarian and/or fallopian tube, thereby compromising vascular perfusion and potentially culminating in ischemia and necrosis [1, 2]. This medical entity primarily impacts reproductive-aged individuals, often presenting with nonspecific clinical manifestations, which subsequently impedes timely diagnosis. Consequently, expeditious operative management is paramount for safeguarding gonadal function and mitigating the development of severe adverse sequelae, including hemorrhagic infarction [3].

Diagnostic imaging modalities are paramount in establishing the diagnosis of adnexal torsion [4]. While ultrasonography is frequently employed as the initial diagnostic imaging modality, it nevertheless exhibits notable constraints concerning its diagnostic performance. Specifically, its reported sensitivity, ranging from 46% to 73%, and its specificity can be suboptimal, particularly in differentiating torsion from other acute intra-abdominal pathologies [5]. Computed Tomography (CT), an imaging modality employed for the assessment of acute abdominal pathologies,

MSW MANAGEMENT -Multidisciplinary, Scientific Work and Management Journal
ISSN: 1053-7899
Vol. 35 Issue 2, 2025, Pages: 2202-2211

presents several notable disadvantages. Firstly, it necessitates patient exposure to ionizing radiation, which carries inherent risks of adverse health effects. Secondly, it exhibits suboptimal contrast differentiation. Furthermore, CT scans demonstrate diminished diagnostic precision for the identification of torsion, achieving an accuracy rate of merely 42%. Moreover, its utility is constrained in the comprehensive evaluation of neoplastic masses that are co-occurring with or causally linked to torsion [6].

Magnetic Resonance Imaging (MRI) furnishes excellent soft tissue demarcation and permits comprehensive characterization of the adnexal structures, consequently assisting in the accurate identification of torsion and its associated sequelae [7]. Existing scholarship is limited regarding the application of magnetic resonance imaging (MRI) for the diagnosis of adnexal torsion. These investigations have evaluated various MRI characteristics, including the manifestation of ascites, uterine displacement, mural thickening discernible on T2-weighted imaging (T2WI), the presence of a twisted pedicle, signal alterations on T1-weighted imaging (T1WI) and diffusion-weighted imaging (DWI), diminished or absent contrast enhancement, and perifollicular hemorrhage [8]. A significant proportion of these investigations employed an extensive pelvic magnetic resonance imaging (MRI) methodology, frequently involving the administration of contrast agents to assess ovarian viability [9]. Nevertheless, this particular diagnostic strategy can necessitate substantial temporal resources, especially in urgent clinical scenarios.

In response to this deficiency, our investigation examines the implementation of an ultra-short, optimized magnetic resonance imaging (MRI) protocol, specifically conceived to accelerate image acquisition while preserving diagnostic fidelity. Previous investigations have established the efficacy of abbreviated MRI sequences across various acute clinical scenarios, implying their potential benefit within the context of adnexal torsion. This streamlined protocol endeavors to furnish a prompt yet dependable assessment of the adnexal structures, thereby facilitating expeditious surgical intervention when medically indicated.

Furthermore, a robust MRI-based scoring framework can augment clinical decision-making by accurately prognosticating the extent of ovarian compromise. Such a system is instrumental in guiding surgical planning regarding the immediacy and scope of operative management, with the potential to ameliorate patient outcomes. Prior scholarly work has underscored the diagnostic significance of specific MRI characteristics, including interstitial edema, hemorrhage, and reduced perfusion, for identifying adnexal torsion and its associated complications. Our current study extends this knowledge by validating an optimized scoring rubric specifically adapted for application with an ultra-short MRI regimen.

AIM: To evaluate the diagnostic accuracy of an MRI scoring system (ultra-short, optimized MRI protocol) in predicting haemorrhagic necrosis in adnexal torsion.

OBJECTIVES:

1. To describe the radiological characteristics of ovarian/adnexal torsion undergoing surgery in a tertiary care centre.
2. To determine the diagnostic accuracy of an MRI scoring system (ultra-short, optimized MRI protocol) in predicting haemorrhagic necrosis in adnexal torsion in comparison with intraoperative and/or histopathological evidence of haemorrhagic necrosis.

METHODOLOGY:

Study design, setting, and duration:

This empirical investigation employed a cross-sectional study design and was undertaken at a tertiary care hospital. The research spanned twelve months, from February 2024 to February 2025. The study was conducted in the Department of Radiology at the Chettinad Hospital and Research Institute, part of the Chettinad Academy of Research and Education, located in Chennai, India.

Study population:

All patients undergoing magnetic resonance imaging (MRI) in the Department of Radiology at Chettinad Hospital and Research Institute, Chettinad Academy of Research and Education, were incorporated, contingent upon adherence to established inclusion and exclusion criteria.

Inclusion criteria:

Female patients between 10 and 50 years of age, presenting with ovarian/adnexal torsion (in magnetic resonance imaging), with MRI diagnosis of ovarian/adnexal torsion, undergoing surgery and those willing to provide informed written consent were included in the study.

Exclusion criteria:

Patients with MRI diagnosis excluding torsion and undergoing surgery/histopathological evaluation elsewhere were excluded from the study.

Sampling technique:

For this study, subjects were selected using a non-probability sampling - convenience sampling technique, from individuals encountered at the designated study setting.

Sample size:

An observational retrospective study by Renganathan et al. [10] among individuals diagnosed with ovarian/adnexal torsion via magnetic resonance imaging (MRI) revealed that 58.1% exhibited intraoperative or pathological indications of hemorrhagic necrosis. Considering a Type I error rate (alpha) of 5%, a statistical power set at 80% (corresponding to a Type II error rate or beta of 20%), an absolute margin of error (precision) of 10%, and an anticipated participant attrition rate (non-response rate) of 10%. Accounting for these parameters, the minimum necessary sample size was approximated at **50 patients**, calculated to achieve the specified power and an 80% confidence level for the estimated proportion.

MSW MANAGEMENT -Multidisciplinary, Scientific Work and Management Journal
ISSN: 1053-7899
Vol. 35 Issue 2, 2025, Pages: 2202-2211

The formula used for calculating sample size was:

$$n = \frac{z^2pq}{d^2}$$

where:
n = required sample size
z = standard normal variate for a 5% significance level
p = prevalence
q = 100-p
d = absolute precision

Procedure:

The methodological design of the current study is delineated in the flowchart (Image 1). Participants meeting the predefined eligibility criteria were subsequently enrolled in the investigation. Prior to their involvement, comprehensive informed consent was obtained from each participant's legal guardian, rendered in their native language, following a detailed exposition of the study's objectives and procedures.

Magnetic Resonance (MR) imaging data were acquired using a Philips 3.0-Tesla (3T) MR system outfitted with a conventional eight-channel quadrature head coil. Furthermore, scans were predominantly conducted utilizing a 3.0-Tesla (3T) Siemens Skyra MRI unit. A single gestational participant, however, underwent imaging on a 1.5-Tesla (1.5T) Philips Ingenia MRI unit, which employed a phased-array coil. To mitigate head motion, all participants were positioned in a supine position and secured with customized stabilizing apparatus.

For individuals primarily referred for pelvic MR imaging due to equivocal ultrasonographic findings originating from external institutions, an extensive MR imaging protocol was implemented. This encompassed axial T1-weighted sequences, multi-planar T2-weighted sequences, axial diffusion-weighted imaging (DWI), and both pre- and post-contrast administration T1-weighted fat-saturated sequences. Conversely, a limited MR imaging protocol, comprising T2-weighted sequences in either two or three orthogonal planes, was applied to participants presenting with non-definitive ultrasonographic results generated by our internal facility.

MRI data acquisition utilized sequences characterized by a 3 mm slice thickness and a 1 mm interslice gap. The temporal duration of both comprehensive and abbreviated MRI examinations was systematically documented from the Picture Archiving and Communication System (PACS).

Three independent observers performed an analysis of the MRI images and subsequently reported their findings. These observations encompassed findings such as pedicle torsion (defined as a twisting of the pedicle), diminished signal intensity (hypointensity) within the ovarian stroma, adjacent to the follicle, within the cyst wall or ovarian capsule, and affecting the pedicle itself. Furthermore, the thickness of the cyst wall was assessed when known, utilizing a 3 mm threshold to categorize the wall as either thin or thick. The presence of diminished signal intensities at these specified anatomical locations, in conjunction with the measured cyst wall thickness, served as diagnostic indicators for tissue necrosis. For the quantitative assessment of these hypointensities, a binary score (0 or 1) was assigned to each respective anatomical site, indicating the absence or presence of the finding. Each patient subsequently received a cumulative score, ranging from a minimum of 0 to a maximum of 4.Intraoperative observations were meticulously documented from the surgical reports, providing detailed information on ovarian viability and the specific surgical intervention performed. The histopathological examination report comprised observations pertaining to ovarian congestion or hemorrhagic necrosis. Any co-occurring ovarian lesions and their definitive histopathological diagnoses were also systematically recorded.

Fig 1: Flowchart of the study methodology

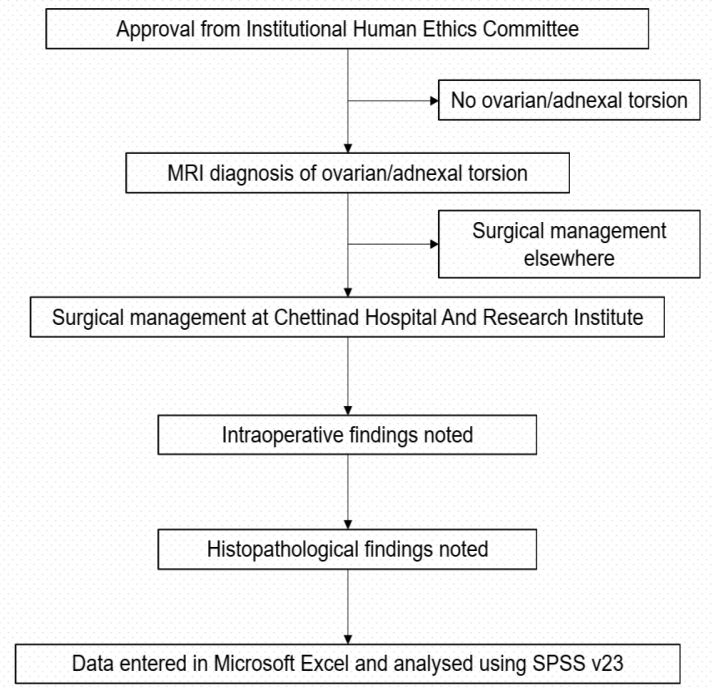

MSW MANAGEMENT -Multidisciplinary, Scientific Work and Management Journal
ISSN: 1053-7899
Vol. 35 Issue 2, 2025, Pages: 2202-2211

Outcomes measured:

a) Primary outcomes:

- Radiological characteristics of ovarian/adnexal torsion (Cause & malignant nature of torsion)
- Diagnostic accuracy of ultra-short, optimized MRI protocol in predicting haemorrhagic necrosis in adnexal torsion

b) Secondary outcomes:

- Age
- Menopausal status

Statistical analysis:

The data acquired were initially compiled using Microsoft Excel and subsequently analysed utilizing the Statistical Package for Social Sciences (SPSS) version 23. Categorical variables were characterized by frequencies (percentages). For continuous variables, descriptive statistics included the mean (with standard deviation) and the median (with interquartile range). Normality testing was conducted using both the Kolmogorov-Smirnov and Shapiro-Wilk tests. The diagnostic accuracy of the optimized, ultra-short MRI protocol—defined by specific imaging markers such as hypointensity of the ovarian stroma, surrounding the follicle, cyst wall, or ovarian capsule, as well as the twisted pedicle and a thickened cyst wall—was ascertained through the calculation of sensitivity, specificity, positive predictive value, and negative predictive value. A p-value of less than 0.05 was considered statistically significant.

Ethical consideration:

Ethical approval was obtained from the Institutional Human Ethics Committee of Chettinad Hospital & Research Institute before the commencement of the study (Ref no: IHEC-I/2484/24). The potential for adverse effects or participant inconvenience arising from this research is considered exceedingly low. In alignment with the standards outlined in the Indian Council of Medical Research – National Ethical Guidelines for Biomedical and Health Research involving Human Participants, this investigation is formally categorized as presenting "less than minimal risk," primarily due to its design as a non-interventional, questionnaire-based study.

RESULTS:

A total of 50 participants were included in the study.

Table 1: Socio-demographic profile of the participants (N=50)

Age-wise distribution		
Age (Years)	**Frequency (n)**	**Percentage (%)**
≤20	8	16.0%
21-30	9	18.0%
31-40	8	16.0%
41-50	25	50.0%
Total	50	100.00%
Age (in years) (Mean SD)		39.5 (7.3)
Menopausal status		
Socio-economic status	**Frequency (n)**	**Percentage (%)**
Prepubertal	7	14.0%
Premenopausal	31	62.0%
Postmenopausal	12	24.0%
Total	50	100.00%

Table 1 shows the socio-demographic profile of the participants. Analysis of the age distribution indicated that the predominant segment of the cohort, comprising 50% (n=25) of individuals, was situated in the 41-50 year age range, thereby suggesting a notable concentration of participants within the more advanced age categories. Stratification by menopausal status demonstrated that 14% (n=7) of the cohort were prepubertal. The premenopausal group constituted the predominant proportion, accounting for 62% (n=31) of the sample, while postmenopausal individuals comprised 24% (n=12). This profile indicates that participants in the premenopausal stage represented the predominant category.

MSW MANAGEMENT -Multidisciplinary, Scientific Work and Management Journal
ISSN: 1053-7899
Vol. 35 Issue 2, 2025, Pages: 2202-2211

Figure 2: Duration for complete MRI study and ultra-short, optimized MRI protocol (N=50)
***p value <0.05 – Statistically significant**

Figure 2 demonstrates the duration taken to complete MRI study and ultra-short, optimized MRI protocol among the study participants. The mean duration to complete a conventional magnetic resonance imaging (MRI)

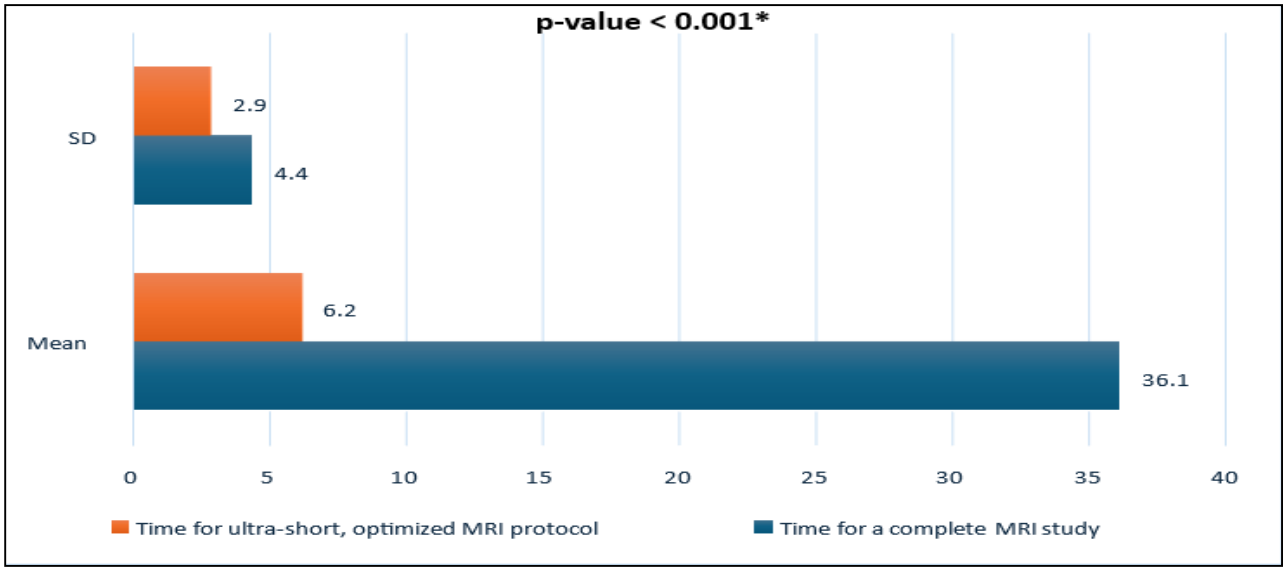

examination was recorded as 36.1 minutes, with a standard deviation of 4.4 minutes. Conversely, the expedited and optimized MRI protocol demonstrated a markedly reduced average duration of 6.2 minutes, with a standard deviation of 2.9 minutes. A statistically significant difference was observed between the two procedural durations ($p < 0.001$), thereby indicating a substantial diminution in acquisition time achieved through the optimized protocol.

Table 2: Distribution of cause and type of torsion (N=50)

Cause of torsion (N=50)		
Cause	**Frequency (n)**	**Percentage (%)**
Known	37	74.0%
Unknown	13	26.0%
Total	50	100.00%
Type of torsion (n=37)		
Type	**Frequency (n)**	**Percentage (%)**
Benign	31	83.8%
Malignant	6	16.2%
Total	37	100.00%

Table 2 shows the distribution of cause and type of torsion in the study population. The underlying etiology of adnexal torsion was known in 74% (n=37) of occurrences, with the cause remaining undetermined in 26% (n=13) of the individuals. Within the cohort of 37 patients where a specific cause was identified, the vast majority (83.8%, n=31) were attributed to benign conditions, while a smaller proportion (16.2%, n=6) stemmed from malignant pathologies.

Table 3: Causes of torsion in known participants (n=37)

Benign causes of torsion (n=31)		
Benign cause	**Frequency (n)**	**Percentage (%)**
Functional cyst	9	29.0%
Dermoid	4	12.9%
Benign serous cyst	4	12.9%
Serous cystadenoma	6	19.4%
Sero mucinous cystadenoma	2	6.5%
Mucinous cystadenoma	2	6.5%

MSW MANAGEMENT -Multidisciplinary, Scientific Work and Management Journal
ISSN: 1053-7899
Vol. 35 Issue 2, 2025, Pages: 2202-2211

Fibroma	1	3.2%
Papillary serous cystadenofibroma and coexisting Brenner tumour	1	3.2%
Para ovarian cyst	2	6.5%
Total	31	100.00%
Malignant causes of torsion (n=6)		
Malignant cause	**Frequency (n)**	**Percentage (%)**
High grade serous carcinoma	2	33.3%
Endometrial adenocarcinoma	3	50.0%
Low-grade serous carcinoma	1	16.7%
Total	6	100.00%

Table 3 enlists the distribution of benign and malignant causes of torsion among the study population. Regarding the 31 individuals diagnosed with benign adnexal torsion, the predominant etiological factor identified was a functional cyst, which constituted 29% (n=9) of the occurrences. This was followed by serous cystadenoma, observed in 19.4% (n=6) of cases. For the 6 patients presenting with malignant torsion, endometrial adenocarcinoma represented the primary underlying pathology, found in 50% (n=3) of these instances.

Table 4: Distribution of patients by intraoperative/pathological evidence of haemorrhagic necrosis (N=50)

Intraoperative/pathological evidence of haemorrhagic necrosis	Frequency (n)	Percentage (%)
Present	29	58.0%
Absent (Viable ovary)	21	42.0%
Total	50	100.0%

Table 4 shows the distribution of patients by intraoperative/pathological evidence of haemorrhagic necrosis. Evaluation conducted either intraoperatively or through subsequent histopathological analysis indicated the presence of hemorrhagic necrosis in 58% (n=29) of the cases. Conversely, 42% (n=21) of the patients exhibited viable ovarian tissue, devoid of any signs of cellular demise.

Table 5: Association between ultra-short, optimized MRI protocol scores and intraoperative/pathological evidence of haemorrhagic necrosis, and various features (N=50)

Ultra-short, optimized MRI protocol	**Intraoperative/pathological evidence of haemorrhagic necrosis**			**p-value**
	Present (n=29)	**Absent (n=21)**	**Total (N=50)**	
	n (%)	**n (%)**	**n (%)**	
2 or more	27 (93.1%)	2 (9.5%)	29 (58.0%)	<0.001*
Less than 2	2 (6.9%)	19 (90.5%)	21 (42.0%)	
Pedicle hypointensity	**Intraoperative/pathological evidence of haemorrhagic necrosis**			**p-value**
	Present (n=29)	**Absent (n=21)**	**Total (N=50)**	
	n (%)	**n (%)**	**n (%)**	
Present	18 (62.1%)	0 (0.0%)	18 (36.0%)	<0.001*
Absent	11 (37.9%)	21 (100.0%)	32 (64.0%)	
Cyst wall hypointensity	**Intraoperative/pathological evidence of haemorrhagic necrosis**			**p-value**

MSW MANAGEMENT -Multidisciplinary, Scientific Work and Management Journal
ISSN: 1053-7899
Vol. 35 Issue 2, 2025, Pages: 2202-2211

	Present (n=29)	Absent (n=21)	Total (N=50)	
	n (%)	n (%)	n (%)	
Present	26 (89.7%)	4 (19.0%)	30 (60.0%)	<0.001*
Absent	3 (10.3%)	17 (81.0%)	20 (40.0%)	
Perifollicular hypointensity	**Intraoperative/pathological evidence of haemorrhagic necrosis**			**p-value**
	Present (n=29)	**Absent (n=21)**	**Total (N=50)**	
	n (%)	**n (%)**	**n (%)**	
Present	21 (72.4%)	7 (33.3%)	28 (56.0%)	<0.006*
Absent	8 (27.6%)	14 (66.7%)	22 (44.0%)	
Stromal hypointensity	**Intraoperative/pathological evidence of haemorrhagic necrosis**			**p-value**
	Present (n=29)	**Absent (n=21)**	**Total (N=50)**	
	n (%)	**n (%)**	**n (%)**	
Present	18 (62.1%)	1 (4.8%)	19 (38.0%)	<0.001*
Absent	11 (37.9%)	20 (95.2%)	31 (62.0%)	
Cyst wall thickness	**Intraoperative/pathological evidence of haemorrhagic necrosis**			**p-value**
	Present (n=29)	**Absent (n=21)**	**Total (N=50)**	
	n (%)	**n (%)**	**n (%)**	
Thick	9 (31.0%)	2 (9.5%)	11 (22.0%)	0.069
Thin	20 (69.0%)	19 (90.5%)	39 (78.0%)	

***p value <0.05 – Statistically significant**

Table 5 compares the association between ultra-short, optimized MRI protocol scores and intraoperative/pathological evidence of haemorrhagic necrosis with various features of torsion. Among the group of 29 individuals confirmed to have haemorrhagic necrosis, a substantial majority (93.1%, n=27) registered an MRI score of 2 or higher. Conversely, within the 21-patient cohort lacking evidence of haemorrhagic necrosis, a predominant proportion (90.5%, n=19) presented with a score below 2. This observed relationship achieved statistical significance ($p < 0.001$), thereby underscoring a strong predictive association where elevated MRI scores are profoundly linked to the presence of haemorrhagic necrosis.

Pedicle hypointensity was identified in a substantial majority (62.1%, n=18) of individuals exhibiting haemorrhagic necrosis, demonstrating a highly statistically significant association ($p < 0.001$). Furthermore, cyst wall hypointensity was detected in a considerable proportion (89.7%, n=26) of cases with haemorrhagic necrosis, also indicating a highly significant correlation (= < 0.001).

Perifollicular hypointensity was evident in nearly three-quarters (72.4%, n=21) of patients with haemorrhagic necrosis, with this disparity also reaching statistical significance ($p = 0.006$). Stromal hypointensity was manifested in 62.1% (n=18) of individuals with haemorrhagic necrosis, establishing a highly robust association ($p < 0.001$). While increased cyst wall thickness was noted more frequently in patients with haemorrhagic necrosis (31%, n=9), this particular association did not achieve statistical significance ($p = 0.069$).

MSW MANAGEMENT -Multidisciplinary, Scientific Work and Management Journal
ISSN: 1053-7899
Vol. 35 Issue 2, 2025, Pages: 2202-2211

Table 6: Diagnostic accuracy of ultra-short, optimized MRI protocol parameters in predicting haemorrhagic necrosis in adnexal torsion (N=50)

	Sensitivity (%)	Specificity (%)	PPV (%)	NPV (%)
Pedicle hypointensity	62.1	100	100	65.6
Cyst wall hypointensity	89.7	81.0	86.7	85.0
Perifollicular hypointensity	72.4	66.7	75.0	63.6
Stromal hypointensity	62.1	95.2	94.7	64.5
Cyst wall thickness	31.0	90.5	81.8	48.7
Ultra-short, optimized MRI protocol – scores 2 or more	93.1	90.5	93.1	90.5

Table 6 shows the various parameters used to assess the diagnostic accuracy of the ultra-short, optimized magnetic resonance imaging (MRI) protocol for identifying haemorrhagic necrosis in cases of adnexal torsion.

The comprehensive MRI scoring protocol, where a diagnostic threshold of two or more points was applied, demonstrated robust diagnostic performance. This was evidenced by a sensitivity of 93.1%, a specificity of 90.5%, a positive predictive value (PPV) of 93.1%, and a negative predictive value (NPV) of 90.5%. These metrics collectively indicate its utility as a dependable instrument for the prognostication of hemorrhagic necrosis in adnexal torsion.

DISCUSSION:

The present investigation aimed to determine the diagnostic efficacy of an ultra-short, optimized magnetic resonance imaging (MRI) scoring system for predicting hemorrhagic necrosis in cases of adnexal torsion. The findings offer valuable insights into the performance of the optimized MRI protocol, demographic profile, etiology, and the characteristics of adnexal torsion. A central outcome of this research was the significant curtailment of MRI scan acquisition time achieved through the optimized protocol. Specifically, the mean duration for a complete MRI study was reduced from 36.1 minutes to 6.2 minutes using the ultra-short protocol. This abbreviation is congruent with previous research by Renganathan et al. [10], which demonstrated that condensed MRI protocols can maintain high diagnostic accuracy while enhancing workflow efficiency. This expedited scan time not only facilitates more rapid diagnosis but also contributes to improved patient comfort and more efficient resource utilization within radiology departments. Furthermore, Lee et al. [11] highlighted the critical importance of time-efficient imaging regimens, particularly in acute settings like adnexal torsion in pregnancy, where prompt clinical decision-making is paramount.

The average age of participants was 39.5 years, with half of the individuals between 41 and 50 years. This demographic pattern is consistent with the established epidemiology of adnexal torsion, which primarily impacts females during their reproductive years, as highlighted by Khalil & El-Dieb. [12] A significant majority (62%) of the study cohort was premenopausal, a finding that corroborates the elevated incidence of functional ovarian cysts and other benign adnexal masses in this age demographic, which inherently predispose individuals to torsional events, as stated by Wattar et al. [13]

The causative factor was known in a substantial proportion (74%) of the torsion cases within this investigation. Non-malignant lesions constituted the overwhelming majority (83.8%) of these identified causes, while neoplastic etiologies accounted for 16.2%. Among the benign origins, functional cysts were the predominant factor (29%), followed by serous cystadenoma (19.4%). The current findings substantiate prior investigation by Asfour et al. [14], which have consistently demonstrated that benign ovarian neoplasms constitute the predominant causative agents in adnexal torsion. The discernment of malignant pathologies, especially aggressive neoplastic entities, highlights the critical importance of accurate pre-operative diagnostic assessment to inform optimal surgical strategies and subsequently ameliorate patient prognoses, as signified by Huang et al. [15]

This investigation assessed the predictive efficacy of an ultra-short, optimized magnetic resonance imaging assessment tool in identifying hemorrhagic necrosis in cases of adnexal torsion. Pedicle hypointensity was evident in 62.1% of patients presenting with hemorrhagic necrosis and was entirely absent in those devoid of necrosis. This robust correlation is consistent with prior research conducted by Özdemir et al. [16] that has underscored the compromised pedicle as a pivotal determinant of both the extent of torsional damage and subsequent ovarian viability. The consistent absence of pedicle hypointensity in patients devoid of necrosis suggests that this MRI characteristic exhibits a high degree of specificity for prognosticating tissue necrosis, thereby establishing it as a significant indicator in clinical evaluations.

MSW MANAGEMENT -Multidisciplinary, Scientific Work and Management Journal
ISSN: 1053-7899
Vol. 35 Issue 2, 2025, Pages: 2202-2211

Cyst wall hypointensity was observed in a substantial majority (89.7%) of patients presenting with hemorrhagic necrosis, in stark contrast to its significantly lower prevalence (19%) among individuals without this condition. This observation is consistent with the findings of Chen et al. [17], whose research indicated that both cyst wall thickening and aberrant signal intensity on magnetic resonance imaging (MRI) serve as reliable indicators of compromised ovarian tissue. Consequently, the pronounced diagnostic utility of cyst wall hypointensity, evidenced by its high sensitivity and specificity in the current investigation, underscores its reliability as a prognostic marker for necrosis.

Perifollicular hypointensity was observed in a substantial majority (72.4%) of patients presenting with haemorrhagic necrosis, in contrast to approximately one-third (33.3%) of those without this condition. This noteworthy association is corroborated by the findings of Moribata et al. [18] who demonstrated that perifollicular haemorrhage, as detected by magnetic resonance imaging (MRI), exhibits a strong correlation with histopathological evidence of necrosis. Accordingly, the presence of perifollicular hypointensity signifies underlying hemorrhagic alterations, furnishing clinicians with vital information regarding ovarian viability and the expediency of therapeutic intervention.

Stromal hypointensity was detected in a significant proportion (62.1%) of cases exhibiting hemorrhagic necrosis, whereas it was observed in a markedly lower percentage (4.8%) among those without this condition. This observation is consistent with the findings of Chiou et al. [19], who established that stromal alterations visible on magnetic resonance imaging serve as dependable markers of tissue necrosis in adnexal torsion. The substantial specificity (95.2%) and positive predictive value (94.7%) associated with stromal hypointensity underscore its utility in differentiating between viable and non-viable ovarian parenchyma.

While a greater cyst wall thickness was observed in 31% of patients exhibiting hemorrhagic necrosis, compared to 9.5% of those without, this association did not attain statistical significance. This aligns with findings of a study conducted by Noda et al. [20], who reported that larger cyst dimensions and increased mural thickness are linked to an elevated risk of torsion and necrosis. However, the lack of statistical significance in the current investigation suggests that isolated cyst wall thickness may not be a conclusive predictor of necrosis, thereby emphasizing the necessity of evaluating this parameter alongside other magnetic resonance imaging characteristics.

The refined magnetic resonance imaging (MRI) assessment system, which synthesizes the aforementioned imaging characteristics, exhibited superior diagnostic precision. A threshold score of two or higher within this system demonstrated a robust association with the presence of hemorrhagic tissue death, yielding a sensitivity of 93.1%, a specificity of 90.5%, a positive predictive value of 93.1%, and a negative predictive value of 90.5%. These quantitative metrics affirm the system's significant effectiveness in distinguishing between devitalized and viable ovarian tissue. Furthermore, Rougier et al. [21] reported comparable diagnostic accuracy utilizing an MRI-based classification methodology, thereby reinforcing the practical value of such strategies in clinical environments.

LIMITATIONS:

The limitations of this study on predicting haemorrhagic necrosis in adnexal torsion using an ultra-short MRI protocol include: Being a single-center study, its findings may not apply broadly. It did not integrate MRI with other common modalities like ultrasound, which could have provided a more thorough and accurate diagnosis. MRI results might be interpreted differently by various observers, especially for subtle signs, and this consistency was not assessed; thus, accuracy might depend on the radiologist's experience. The study did not extensively consider how patient factors like body mass index (BMI), chronic illnesses, or pre-existing gynecological conditions could affect MRI accuracy or the likelihood of necrosis.

Mitigating these limitations in forthcoming studies is anticipated to facilitate the refinement of the diagnostic protocol and bolster its practical applicability.

CONCLUSION:

This study establishes that the ultra-short and optimized MRI protocol serves as an exceptionally effective diagnostic tool to predict haemorrhagic necrosis in adnexal torsion. The considerably reduced imaging acquisition time, complemented by the superior diagnostic accuracy of particular MRI characteristics, specifically hypointensity observed within the pedicle, cyst wall, perifollicular structures, and stroma, emphasizes its potential as a swift and dependable diagnostic modality in acute clinical settings.

Forthcoming studies are anticipated to facilitate the refinement of the diagnostic protocol and bolster its practical applicability.

REFERENCES:

1. Huchon C, Panel P, Kayem G, Schmitz T, Nguyen T, Fauconnier A. Does this woman have adnexal torsion? Human reproduction. 2012;27(8):2359-64.
2. Sasaki KJ, Miller CE. Adnexal torsion: review of the literature. Journal of minimally invasive gynecology. 2014;21(2):196-202.
3. Huchon C, Fauconnier A. Adnexal torsion: a literature review. European Journal of Obstetrics & Gynecology and Reproductive Biology. 2010;150(1):8-12.
4. Dawood MT, Naik M, Bharwani N, Sudderuddin SA, Rockall AG, Stewart VR. Adnexal Torsion: Review of Radiologic Appearances. Radiographics. 2021;41(2):609-24.
5. Wilkinson C, Sanderson A. Adnexal torsion -- a multimodality imaging review. Clin Radiol. 2012;67(5):476-83.

MSW MANAGEMENT -Multidisciplinary, Scientific Work and Management Journal
ISSN: 1053-7899
Vol. 35 Issue 2, 2025, Pages: 2202-2211

6. Chiou SY, Lev-Toaff AS, Masuda E, Feld RI, Bergin D. Adnexal torsion: new clinical and imaging observations by sonography, computed tomography, and magnetic resonance imaging. J Ultrasound Med. 2007;26(10):1289-301.
7. Béranger-Gibert S, Sakly H, Ballester M, Rockall A, Bornes M, Bazot M, et al. Diagnostic Value of MR Imaging in the Diagnosis of Adnexal Torsion. Radiology. 2016;279(2):461-70.
8. Petkovska I, Duke E, Martin DR, Irani Z, Geffre CP, Cragun JM, et al. MRI of ovarian torsion: Correlation of imaging features with the presence of perifollicular hemorrhage and ovarian viability. Eur J Radiol. 2016;85(11):2064- 71.
9. Gopireddy DR, Virarkar M, Kumar S, Vulasala SSR, Nwachukwu C, Lamsal S. Acute pelvic pain: A pictorial review with magnetic resonance imaging. J Clin Imaging Sci. 2022;12:48.
10. Renganathan R, Subramaniam P, Deebika S, Arunachalam VK, Shanmugam J, Cherian M. Scoring system for predicting ovarian necrosis in adnexal torsion using an ultra-short optimized MRI protocol. Abdom Radiol (NY). 2023;48(6):2122-30.
11. Lee JH, Roh HJ, Ahn JW, Kim JS, Choi JY, Lee SJ, et al. The Diagnostic Accuracy of Magnetic Resonance Imaging for Maternal Acute Adnexal Torsion during Pregnancy: Single-Institution Clinical Performance Review. J Clin Med. 2020;9(7).
12. Khalil RM, El-Dieb LR. Sonographic and MRI features of ovarian torsion. The Egyptian Journal of Radiology and Nuclear Medicine. 2016;47(2):621-9.
13. Wattar B, Rimmer M, Rogozinska E, Macmillian M, Khan KS, Al Wattar BH. Accuracy of imaging modalities for adnexal torsion: a systematic review and meta-analysis. BJOG: An International Journal of Obstetrics & Gynaecology. 2021;128(1):37-44.
14. Asfour V, Varma R, Menon P. Clinical risk factors for ovarian torsion. Journal of obstetrics and gynaecology. 2015;35(7):721-5.
15. Huang C, Hong MK, Ding DC. A review of ovary torsion. Ci Ji Yi Xue Za Zhi. 2017;29(3):143-7.
16. Özdemir O, Metin Y, Metin NO, Küpeli A. Contribution of diffusion-weighted imaging to conventional MRI for detection of haemorrhagic infarction in ovary torsion. BMC Med Imaging. 2017;17(1):56.
17. Chen M, Chen C-D, Yang Y-S. Torsion of the previously normal uterine adnexa: evaluation of the correlation between the pathological changes and the clinical characteristics. Acta obstetricia et gynecologica Scandinavica. 2001;80(1):58- 61.
18. Moribata Y, Kido A, Yamaoka T, Mikami Y, Himoto Y, Kataoka M, et al. MR imaging findings of ovarian torsion correlate with pathological hemorrhagic infarction. J Obstet Gynaecol Res. 2015;41(9):1433-9.
19. Chiou S-Y, Lev-Toaff AS, Masuda E, Feld RI, Bergin D. Adnexal torsion: new clinical and imaging observations by sonography, computed tomography, and magnetic resonance imaging. Journal of Ultrasound in Medicine. 2007;26(10):1289-301.
20. Noda Y, Goshima S, Kawada H, Kawai N, Koyasu H, Matsuo M. Preoperative Magnetic Resonance Imaging Diagnosis of Ovarian Torsion. I J Radiol. 2018;15(1):e14270.
21. Rougier E, Mar W, Della Valle V, Morel B, Irtan S, Audureau E, et al. Added value of MRI for the diagnosis of adnexal torsion in children and adolescents after inconclusive ultrasound examination. Diagnostic and Interventional Imaging. 2020;101(11):747-56.